

NERV++: AN ENHANCED IMPLICIT NEURAL VIDEO REPRESENTATION

Ahmed Ghorbel¹ Wassim Hamidouche^{1,2} Luce Morin¹

¹ Univ Rennes, INSA Rennes, CNRS, IETR – UMR 6164, F-35000 Rennes, France

² Technology Innovation Institute P.O.Box: 9639, Masdar City Abu Dhabi, UAE

ABSTRACT

Neural fields, also known as implicit neural representations (INRs), have shown a remarkable capability of representing, generating, and manipulating various data types, allowing for continuous data reconstruction at a low memory footprint. Though promising, INRs applied to video compression still need to improve their rate-distortion performance by a large margin, and require a huge number of parameters and long training iterations to capture high-frequency details, limiting their wider applicability. Resolving this problem remains a quite challenging task, which would make INRs more accessible in compression tasks. We take a step towards resolving these shortcomings by introducing neural representations for videos (NeRV)++, an enhanced implicit neural video representation, as more straightforward yet effective enhancement over the original NeRV decoder architecture, featuring separable conv2d residual blocks (SCRBs) that sandwiches the upsampling block (UB), and a bilinear interpolation skip layer for improved feature representation. NeRV++ allows videos to be directly represented as a function approximated by a neural network, and significantly enhance the representation capacity beyond current INR-based video codecs. We evaluate our method on UVG, MCL_JVC, and Bunny datasets, achieving competitive results for video compression with INRs. This achievement narrows the gap to autoencoder-based video coding, marking a significant stride in INR-based video compression research.

Index Terms— Neural Video Compression, Implicit Neural Representations, Separable Convolution.

1. INTRODUCTION

The proliferation of digital video content in various domains, ranging from entertainment and education to surveillance and remote communication, has spurred intensive research into efficient video processing and compression techniques. In this era, conventional methods, based on established video coding standards such as high-efficiency video coding (HEVC)/H.265 [1] and versatile video coding (VVC)/H.266 [2], have made notable progress in minimizing spatial and temporal redundancies, facilitating efficient storage and transmission of video data. Nevertheless,

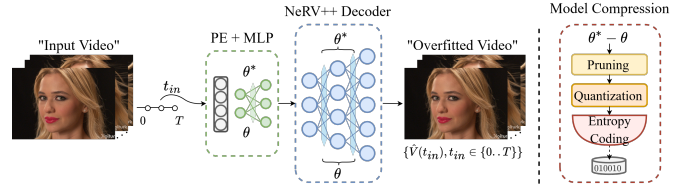


Fig. 1. High-level diagram of implicit neural representation for video compression.

the growing demand for high-quality video streaming, real-time applications, and immersive experiences requires the exploration of innovative approaches to video representation.

In response to these challenges, the advent of learned video compression (LVC) techniques, driven by deep neural networks (DNNs), has ushered in a paradigm shift. These methods leverage the power of artificial intelligence (AI) to learn intricate patterns within video data, enabling adaptive compression schemes tailored to the content's complexity. Several data-driven attempts utilizing convolution network (ConvNet) and autoencoder architectures to compress video signals have been made [3, 4]. These approaches assume that shared decoder networks only need to store or transmit essential video information. Specifically, the encoder generates latent representations of a sequence of frames, which are then quantized and entropy-coded. The decoder subsequently reconstructs an approximate version of the original sequence. This approach often includes temporal consistency priors by selecting key frames within a group of frames and encoding information to reconstruct the remaining frames separately. Several works build on this approach, proposing different forms of representation for the key and predicted frames [5–7]. For instance, the deep video compression (DVC) method proposed by Lu *et al.* [4] has demonstrated compression ratios comparable to or slightly better than software implementations x264 and x265 of advanced video coding (AVC)/H.264 [8] and HEVC/H.265 [9] standards. This redefines the compression pipeline using neural networks instead of hand-crafted algorithms. However, these autoencoder-based approaches are inherently susceptible to biases present in their training datasets and pose challenges due to their extensive parameterization. Learned decoders,

often comprising millions of parameters and requiring up to a million multiplication-accumulation (MAC) operations to decode a single pixel, are several orders of magnitude more complex than conventional counterparts. This complexity poses a potential hindrance to their widespread adoption, despite their promising compression capabilities [3, 4].

In recent years, implicit neural representations (INRs), particularly models like DeepSDF [10], neural radiance field (NeRF) [11], and their derivatives, have played a crucial role in revolutionizing 3D object modeling and image synthesis. They have demonstrated significant success in 3D reconstruction [12, 13] and novel view synthesis applications [14–17], leveraging their compactness and expressiveness. Implemented through neural networks, these INRs offer continuous signal representations, providing versatility by allowing training directly on samples from the signal to be fit (e.g., mapping (x, y) coordinates to RGB color values for images) or through outputs from differentiable processes, as exemplified by NeRF. The capability to parameterize continuous 3D representations positions INRs as a pivotal technology in modern computational 3D and image processing fields. However, these networks encounter the spectral bias issue, struggling to capture high-frequency details. Solutions like SIREN, proposed by Sitzmann *et al.* [18], use periodic activation functions to mitigate this issue, offering improved representation of images and videos. Additionally, Mildenhall *et al.* [11] applied positional encoding, mapping input coordinates to higher dimensions using sinusoidal functions, thereby enhancing the network’s capability to capture fine details. Our work also integrates positional encoding, aligning with recent advancements in INR-based video compression.

In the realm of image compression using INR, an image is conceptualized as a function $f(x, y) = (R, G, B)$, approximated by fitting a neural network to a set of pixels $P = (x, y), (R, G, B)$. The image is then effectively stored in the neural network’s parameters and can be recovered by performing forward passes. Notably, the use of INR frames image compression as a neural network compression problem. The pioneering work by Dupont *et al.* [19] in applying INR to image compression marked a significant advancement in this field. Leveraging SIREN-based models, Sitzmann *et al.* [18] demonstrated the efficiency of INR over JPEG in low-bitrate scenarios. Their approach involved fitting a neural network to an image and compressing it through post-training quantization. Strümpler *et al.* [20] and Dupont *et al.* [21] furthered this research by introducing a meta-learned model at the receiver side and explicit quantization methods. These approaches achieved favorable results by learning and transmitting only the network modulations, then fine-tuning for performance recovery. Their research also explored the implementation of $L1$ regularization to potentially reduce entropy within the weights. However, adjusting the intensity of this regularization displayed only negligible changes in the efficiency of the compressed output. This observation led to the

conclusion that $L1$ regularization might not effectively serve as a mechanism for minimizing entropy in such contexts.

All the aforementioned INR approaches are pixel-based implicit representations, when handling extensive and high-resolution datasets, they exhibit limitations in training and testing time efficiency, rendering them suboptimal for various applications. Conversely, neural representations for videos (NeRV) [22] introduces an image-based implicit representation strategy, integrating convolutional operations with INR to jointly learn an INR across all pixel values. This approach enhances data processing speed and streamlines model training. While this approach sacrifices spatial continuity, it enables the use of convolutional layers, which are more prevalent and effective in image processing tasks compared to fully connected layers. Thus, video encoding in NeRV [22] involves fitting a neural network to frames, with the decoding being a straightforward feedforward process. Initially, the network undergoes training to minimize distortion loss, followed by procedures aimed at diminishing its size, such as converting its weights to an 8-bit floating-point format, alongside quantization and pruning techniques. Their results show that image-based neural video representations can provide superior performance than pixel-based representations for the task of video compression. Additionally, training and inference times are significantly reduced.

Li *et al.* [23] furthered the NeRV [22] approach and proposed E-NeRV, an optimization to this architecture, by segregating spatial and temporal input coordinates. Thereby reducing reliance on large fully connected layers required by NeRV, resulting in a more efficient allocation of network parameters. Recently, Bai *et al.* proposed PS-NeRV [24], a patch-wise approach to video representation using INRs, including adaptive instance normalization (AdaIN) for feature enhancement and capturing high-frequency details. Further, Lee *et al.* [25] proposed FFNeRV that leverages optical flows to exploit temporal redundancies, and adopted multi-resolution temporal grids for mapping continuous temporal coordinates and employing compact convolutional designs with group and pointwise convolutions. Later, Chen *et al.* proposed H-NeRV [26] a hybrid neural representation for videos, advancing beyond standard INRs like NeRV and E-NeRV by incorporating learnable, content-adaptive embeddings. More recently, Kwan *et al.* introduced HiNeRV [27], a novel approach to learning-based video compression by leveraging hierarchical encoding and a sophisticated architecture combining bilinear interpolation, depth-wise convolutional, and multi-layer perceptron (MLP) layers. Finally, Maya *et al.* [28] employed a patch-wise autoregressive design through an INR framework namely NIRVANA, enabling efficient scaling with video resolution and length, and introduces variable bitrate compression that adapts to inter-frame motion.

NeRV and related works [23–27] require the training of networks with different architectures to achieve various rate-distortion (RD) tradeoffs. They apply post-training quantiza-

tion or quantization-aware training (QAT), and weight pruning to achieve compression. Although these approaches have demonstrated fast decoding capability, they still feature a relatively coarse decoder design, imposing limitations on the extraction of relevant video frame features and, consequently, restricting their rate-distortion performance.

One of the main challenges of implicit neural video representation lies in the ability to discern crucial information necessary for video representation, given the constraints imposed by the number of parameters in the decoder blocks. Another significant challenge is that current INR-based models are not explicitly designed with architectural efficiency as a priority and lack the expressiveness needed to represent high-resolution video data at low distortion. This deficiency stems from ineffective decoding blocks, posing a challenge for video compression tasks. While existing approaches strive to enhance training and compression methods, there is a continued need to improve the representation capacity of the decoder network. Lastly, encouraging further exploration of INRs as an alternative to autoencoder-based neural video coding (NVC) is essential to overcome the limitations associated with conventional neural video compression methods. To address these challenges, we present three contributions outlined as follows:

- We have developed a novel compact convolutional architecture for neural video representation, surpassing the representation capacity of state-of-the-art non-hybrid INR-based video codecs. Fig. 1 illustrates a high-level diagram to provide a more comprehensive overview of the proposed framework.
- We have designed the NeRV++ decoder block as a simpler yet effective enhancement over the original NeRV decoder architecture. Our development is characterized by a separable conv2d residual block (SCRB) that encompasses the traditional NeRV upsampling block (UB). Furthermore, we have incorporated a bilinear interpolation layer to refine the feature representation capabilities of the decoder block. This design represents a technical leap forward, offering a more efficient solution for advanced video compression.
- We have conducted extensive experiments on key benchmark datasets for the video compression task. NeRV++ exhibits competitive qualitative and quantitative results compared to previous works and yields high-fidelity time-continuous reconstructions.

Thorough experimentation reveals the effectiveness of the NeRV++ decoder architecture, incorporating separable convolutions, residual connections, and bilinear interpolation layers. These experiments affirm that the NeRV++ framework delivers significant advances in compression efficiency.

The rest of this paper is organized as follows. First, the proposed NeRV++ framework is described in detail in Section 2. Next, we dedicate Section 3 to describing and analyzing the experimental results. Finally, Section 4 concludes the paper and outlines some limitations of this work.

2. PROPOSED NERV++ FRAMEWORK

Our work comprises two proposals for improving neural representations for video compression: a more efficient neural network architecture for video compression (Sec. 2.1) and the formalization of the task as a RD problem (Sec. 3.2). Fig. 1 illustrates an overview of the proposed INR for video compression, named NeRV++. Given a time coordinate t_{in} , the positional encoding (PE) with the MLP decode the time coordinate and output a corresponding feature vector. This embedding is then forwarded to a set of sequential NeRV++ blocks to decode the frame at the corresponding time t_{in} . This overfitted model on the input video sequence is pruned, then quantized, and finally entropy-coded to produce the final compressed video bitstream.

2.1. NeRV++ Overall Architecture

Given an input raw video $V(t_{in}), t_{in} \in 0 \dots T$, our goal is to find a continuous representation for the video. The representation interprets an arbitrary time coordinate t_{in} into an *RGB* video frame. To achieve this, we introduce an enhanced implicit neural video representation, NeRV++. It enables time-continuous neural video representation and is parameterized by MLPs and NeRV++ decoder blocks, taking the form: $\hat{V}(t_{in}) = f(t_{in})$, where f is the proposed video representation defined by the encoded feature and network parameters. t_{in} is the temporal coordinate, and $\hat{V}(t_{in})$ is the predicted *RGB* frame at the instant t_{in} , as depicted in Fig. 1.

The overall pipeline of the proposed solution is illustrated in Fig. 2. The framework comprises three modular parts. First, the shallow feature extraction consists of a positional encoding operation and a small MLP. Second, the NeRV++ decoder consists of a combination of separable conv2d residual blocks that sandwich the upsampling layers. We insert a bilinear interpolation skip connection between these layers for feature refinement. Finally, the convolutional head, coupled with a Tanh activation function, performs the final projection. This architecture enables the model to learn weights that achieve high-accuracy video representations and maintain low entropy, optimizing for compression efficiency.

Globally, the SCRb incorporates a series of architectural choices from a Swin Transformer [29] while maintaining the network’s simplicity as a standard ConvNet without introducing any attention-based modules. These design decisions can be summarized as follows: macro design, ResNeXt’s grouped convolution, inverted bottleneck, large kernel size, and various layer-wise micro designs. In Fig. 2, we illustrate the

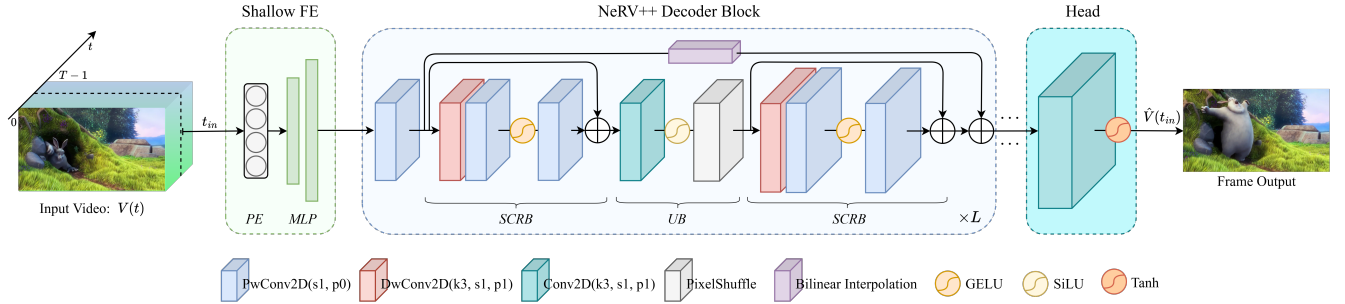


Fig. 2. Overall NeRV++ framework. We illustrate the video compression diagram of our NeRV++. PE for positional encoding, MLP for multilayer perceptron, **scrb!** stands for the separable conv2d residual block, and UB for upsampling block.

SCRB block, where $\text{DwConv2D}(\cdot)$ refers to depthwise 2D convolution, $\text{PwConv2D}(\cdot)$ for point-wise 2D convolution, and gaussian error linear unit (GELU) for the activation function. Finally, it is essential to note that we propose to add a residual connection to simplify the learning process, enabling the training of much deeper networks by allowing gradients to flow through the architecture more effectively, thus improving performance without adding complexity.

2.2. Model Compression Pipeline

Model compression is typically achieved through pruning and quantization of network weights. Pruned models contain a majority of zeros and can be stored in sparse matrix formats for model size reduction. Alternatively, quantization works to reduce the number of bits needed to store each model weight, resulting in reduced disk space. As implicit neural networks represent the data using their model weights, data compression translates to model compression. We perform post-hoc pruning and quantization of the model because it has been found that QAT considerably increases training time for a relatively small improvement compared to post-training quantization (PTQ).

Weight pruning. In INR-based methods [22–28], weight pruning is often employed to enhance model compression by globally zeroing weights with the smallest magnitudes, leveraging the principle that these contribute minimally to the model’s output. Specifically, $L1$ unstructured pruning, a technique supported by the PyTorch library [30], applies this concept by targeting individual weights based on their $L1$ norm, promoting a sparse representation without adhering to the structure of channels or layers. Following the pruning process, fine-tuning is essential to recover or boost the model’s performance. This stage adjusts the remaining weights to compensate for the loss induced by pruning, using a reduced learning rate and potentially fewer training epochs. This combined approach of pruning and fine-tuning facilitates the deployment of efficient, compact INR models without significantly sacrificing accuracy, making it ideal for applications in

resource-limited environments. We also evaluated our model with $L1$ unstructured pruning for fair comparisons, eliminating 20% of the total convolutional weights.

Weight quantization and entropy coding. In the domain of INR-based video compression, weight quantization and entropy coding emerge as pivotal techniques for optimizing storage and transmission efficiency [22]. Weights quantization reduces the precision of the neural network’s weights to a limited set of values, thereby decreasing the model’s size and the computational complexity involved in processing video data. This step is crucial for fitting the neural representation within bandwidth constraints while maintaining acceptable video quality. Following quantization, entropy coding is applied to further compress the model by exploiting the statistical dependencies of the quantized weights, encoding them in a more compact form based on their frequency of occurrence. Techniques such as Huffman coding [31] or arithmetic coding [32] are commonly used, efficiently mapping more frequent patterns to shorter codes. Together, weight quantization and entropy coding significantly enhance the compression ratio of INR-based video compression methods, enabling high-quality video to be stored and transmitted with minimal resource usage. To achieve these outcomes, we utilized 8-bit post-training weight quantization coupled with Huffman entropy coding, further refining our compression efficiency.

3. RESULTS AND ANALYSIS

3.1. Experimental Setup

Baselines. We compare our solution with the benchmark INR-based video codecs, including NeRV [22], E-NeRV [23], and PS-NeRV [24].

Datasets. We assessed the performance of our method using seven 1080p videos from the widely utilized UVG video dataset [33], four 720p videos from the MCL_JVC video dataset [34], and one 720p Bunny video from the scikit-

Table 1. PSNR (dB) \uparrow performance on UVG (1080p) dataset of non-hybrid INRs for video compression.

Size	Video Codec	Beauty	Bosph.	Honey.	Jockey	Ready.	Shake.	Yacht.	Average
Small	NeRV	32.83	32.20	38.15	30.30	23.62	33.24	26.43	30.97
	E-NeRV	33.13	33.38	38.87	30.61	24.53	34.26	26.87	31.66
	PS-NeRV	32.94	32.32	38.39	30.38	23.61	33.26	26.33	31.03
	NeRV++	33.48	34.03	38.65	31.87	24.91	33.97	27.37	32.04
	NeRV*++	33.57	34.59	38.76	32.46	25.29	34.11	27.65	32.35
Medium	NeRV	33.67	34.83	39.00	33.34	26.03	34.39	28.23	32.78
	E-NeRV	33.97	35.83	39.75	33.56	26.94	35.57	28.79	33.49
	PS-NeRV	33.77	34.84	39.02	33.34	26.09	35.01	28.43	32.93
	NeRV++	33.90	35.71	39.08	34.33	26.79	34.52	28.79	33.30
	NeRV*++	33.97	36.16	39.15	34.74	27.20	34.60	29.06	33.55
Large	NeRV	34.15	36.96	39.55	35.80	28.68	35.90	30.39	34.49
	E-NeRV	34.25	37.61	39.74	35.45	29.17	36.97	30.76	34.85
	PS-NeRV	34.50	37.28	39.58	35.34	28.56	36.51	30.28	34.58
	NeRV++	34.25	37.47	39.46	36.22	29.23	35.72	30.78	34.72
	NeRV*++	34.28	37.77	39.48	36.45	29.59	35.83	30.99	34.91

video test dataset [35]. This evaluation aimed to compare our approach with other neural field-based video compression methods. The chosen datasets encompass a diverse range of videos, spanning from nearly static scenes to fast-moving sequences.

Implementation details. We implemented all models on PyTorch, and the experimental study was carried out on an RTX 5000 Ti GPU and an Intel(R) Xeon(R) W-2145 @ 3.70GHz CPU. All models were overfitted on the same video sequences from the considered datasets with 300 epochs using the ADAM optimizer with parameters $\beta_1 = 0.9$ and $\beta_2 = 0.999$. The initial learning rate is set to 5×10^{-4} with a cosine learning rate scheduler. We used a weighting between mean absolute error (MAE) and (1-SSIM) to formulate the loss function in *RGB* color space. This loss function is expressed as follows, where \mathbf{x} and $\hat{\mathbf{x}}$ stand for predicted and target frames:

$$\mathcal{L} = 0.7 \times MAE(\mathbf{x}, \hat{\mathbf{x}}) + 0.3 \times [1 - SSIM(\mathbf{x}, \hat{\mathbf{x}})]$$

To cover a wide range of rate and distortion points, for our proposed method and baseline, we trained four models (x-small, small, medium, and large configurations) per video for all considered neural codecs.

Evaluation. The performance metrics are peak signal-to-noise ratio (PSNR) and multi-scale structural similarity index (MS-SSIM) at several coding bitrates. We also calculate the BD-rate savings [36], and compare the model size and inference time to measure the model’s efficiency and complexity.

3.2. Rate-Distortion Coding Performance

In this study, we present an evolution of the NeRV++ architecture, denoted as NeRV*++, which incorporates a modification to its primary SCRb by deepening the feature representation in the second layer. This adjustment is aimed at enhancing the model’s ability to capture intricate details.

To showcase the compression efficiency of our proposed approach, NeRV++, and its evolution, NeRV*++, we give the PSNR results in Table 1 across the UVG (1080p) dataset, comparing with state-of-the-art non-hybrid INR-based video codecs. On average, NeRV*++ achieves a $0.86dB$ enhancement in PSNR compared to NeRV across all UVG videos. In all cases, our method produces visually sharper videos than NeRV and PS-NeRV for equal or smaller bitrates, as represented in Fig. 3. Videos such as ”ShakeNDry” and ”Honeybee” often present challenges to compression algorithms relying on motion estimation, such as HEVC or scale-space flow (SSF). On the other hand, for ”YachtRide,” motion-based descriptors compress the scene well, as most motion vectors are parallel. While our method clearly outperforms NeRV and PS-NeRV in this scene, E-NeRV shows close results for medium and large model configurations.

Considering Table 2, NeRV++ and NeRV*++ significantly outperform the NeRV approach on both evaluated metrics, demonstrating the advantages of the NeRV++ decoder block architecture and the well-engineered design of the SCRb. This establishes new non-hybrid state-of-the-art results for implicit neural video representation.

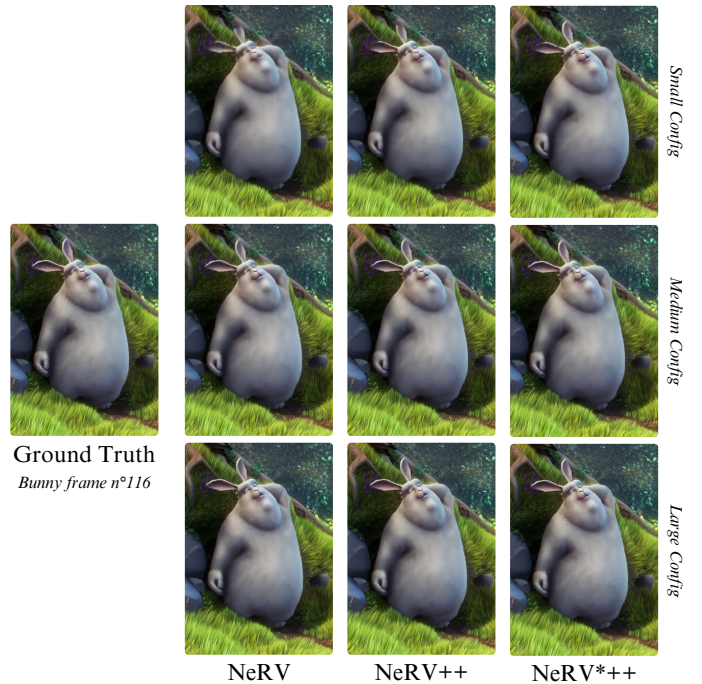


Fig. 3. Visualization of the reconstructed frame number 116 from the Bunny dataset.

3.3. Models Scaling Study

In INR-based approaches, the decoding strategy, which relies on executing a forward pass for each frame independently, significantly enhances the potential for parallel processing in

Table 2. BD-rate \downarrow performance of NeRV++, and NeRV*++ compared to NeRV. Vid. $\{1 \dots 4\}$ are four 720p videos taken from MCLJVC dataset. Bunny is a 720p video from scikit-video test dataset.

Video Codec	Bunny	Vid.1	Vid.2	Vid.3	Vid.4	Average
BD-rate (PSNR dB) \downarrow						
NeRV++	-27.98%	-21.46%	-27.24%	-40.62%	-17.50%	-26.96%
NeRV*++	-25.68%	-24.69%	-30.55%	-26.47%	-16.59%	-24.796%
BD-rate (MS-SSIM dB) \downarrow						
NeRV++	-29.99%	-20.37%	-24.73%	-33.35%	-15.26%	-24.74%
NeRV*++	-25.26%	-22.05%	-28.18%	-26.66%	-13.69%	-23.17%

Table 3. Average decoding latency across 132 frames at 720p resolution, encoded on average at 0.05 bpp.

Video Codec	Latency(fps) \uparrow	#MACs ppx \downarrow	#parameters(M) \downarrow
NeRV	24.89	277.8	5.96
NeRV++ (ours)	15.53	256.3	5.83
NeRV*++ (ours)	10.54	366.8	6.07

the decoding process, thereby improving efficiency. We evaluated the decoding complexity of the proposed method and the NeRV baseline by averaging decoding time across 132 frames at 720p resolution, encoded on average at 0.005 bpp. Table 3 presents the video codec complexity features, displaying the decoding latency (fps), MACs per pixel, and parameter counts for our method compared to the baseline NeRV. Finally, we note that the models were executed using PyTorch on a workstation with one RTX 5000 Ti graphics processing unit (GPU). According to Tables 2 and 3, NeRV++ can achieve significantly better RD performance with a lower MACs per pixel and number of parameters but higher latency on the GPU compared to NeRV. Our findings suggest the potential for significantly reducing decoding times by optimizing the batch size, given adequate GPU memory. This aligns with the observations of Chen *et al.* [22] that INR-based video compression methods outperform alternative models in decoding efficiency.

4. CONCLUSION AND LIMITATIONS

In this study, we introduced the NeRV++ model, an advanced refinement of the NeRV framework aimed at enhancing video compression efficiency. Our innovation lies in the development of a NeRV++ decoder block, which integrates a SCRB around the conventional NeRV upsampling unit, supplemented by a bilinear interpolation layer for improved feature refinement. This configuration not only enhances the architecture but also significantly elevates the performance on 12 videos from UVG, MCLJVC, and Bunny datasets, positioning NeRV++ as a potent solution in the field of video compression technology. While the current findings are encouraging, the practical implementation of neural representa-

tions in video compression as efficient encoders necessitates further investigation into more economical entropy-modeling techniques to enhance encoding efficiency. Additionally, the model complexity and decoding latency still need improvement. It is also possible for the quantized model to outperform the full-precision 32-bit one if the quantized model is initialized with a bigger and deeper model. Besides quantization, other compression techniques like knowledge distillation may also enhance the model compression pipeline.

5. REFERENCES

- [1] Gary J. Sullivan, Jens-Rainer Ohm, Woo-Jin Han, and Thomas Wiegand, "Overview of the high efficiency video coding (hevc) standard," *IEEE Transactions on Circuits and Systems for Video Technology*, vol. 22, no. 12, pp. 1649–1668, 2012.
- [2] Benjamin Bross, Ye-Kui Wang, Yan Ye, Shan Liu, Jianle Chen, Gary J. Sullivan, and Jens-Rainer Ohm, "Overview of the versatile video coding (vvc) standard and its applications," *IEEE Transactions on Circuits and Systems for Video Technology*, vol. 31, no. 10, pp. 3736–3764, 2021.
- [3] Oren Rippel, Sanjay Nair, Carissa Lew, Steve Branson, Alexander G Anderson, and Lubomir Bourdev, "Learned video compression," in *Proceedings of the IEEE/CVF International Conference on Computer Vision*, 2019, pp. 3454–3463.
- [4] Guo Lu, Wanli Ouyang, Dong Xu, Xiaoyun Zhang, Chunlei Cai, and Zhiyong Gao, "Dvc: An end-to-end deep video compression framework," in *Proceedings of the IEEE/CVF Conference on Computer Vision and Pattern Recognition*, 2019, pp. 11006–11015.
- [5] Fabian Mentzer, George Toderici, David Minnen, Sung-Jin Hwang, Sergi Caelles, Mario Lucic, and Eirikur Agustsson, "Vct: A video compression transformer," *arXiv preprint arXiv:2206.07307*, 2022.
- [6] Abdelaziz Djelouah, Joaquim Campos, Simone Schaub-Meyer, and Christopher Schroers, "Neural inter-frame compression for video coding," in *Proceedings of the IEEE/CVF international conference on computer vision*, 2019, pp. 6421–6429.
- [7] Eirikur Agustsson, David Minnen, Nick Johnston, Johannes Balle, Sung Jin Hwang, and George Toderici, "Scale-space flow for end-to-end optimized video compression," in *Proceedings of the IEEE/CVF Conference on Computer Vision and Pattern Recognition*, 2020, pp. 8503–8512.
- [8] Iain E Richardson, *The H. 264 advanced video compression standard*, John Wiley & Sons, 2011.
- [9] Gary J Sullivan, Jens-Rainer Ohm, Woo-Jin Han, and Thomas Wiegand, "Overview of the high efficiency video coding (hevc) standard," *IEEE Transactions on circuits and systems for video technology*, vol. 22, no. 12, pp. 1649–1668, 2012.
- [10] Jeong Joon Park, Peter Florence, Julian Straub, Richard Newcombe, and Steven Lovegrove, "DeepSDF: Learning continuous signed distance functions for shape representation," in *Proceedings of the IEEE/CVF conference on computer vision and pattern recognition*, 2019, pp. 165–174.

- [11] Ben Mildenhall, Pratul P Srinivasan, Matthew Tancik, Jonathan T Barron, Ravi Ramamoorthi, and Ren Ng, “Nerf: Representing scenes as neural radiance fields for view synthesis,” *Communications of the ACM*, vol. 65, no. 1, pp. 99–106, 2021.
- [12] Edgar Sucar, Shikun Liu, Joseph Ortiz, and Andrew J Davison, “imap: Implicit mapping and positioning in real-time,” in *Proceedings of the IEEE/CVF International Conference on Computer Vision*, 2021, pp. 6229–6238.
- [13] Zihan Zhu, Songyou Peng, Viktor Larsson, Weiwei Xu, Hujun Bao, Zhaopeng Cui, Martin R Oswald, and Marc Pollefeys, “Nice-slam: Neural implicit scalable encoding for slam,” in *Proceedings of the IEEE/CVF Conference on Computer Vision and Pattern Recognition*, 2022, pp. 12786–12796.
- [14] Ricardo Martin-Brualla, Noha Radwan, Mehdi SM Sajjadi, Jonathan T Barron, Alexey Dosovitskiy, and Daniel Duckworth, “Nerf in the wild: Neural radiance fields for unconstrained photo collections,” in *Proceedings of the IEEE/CVF Conference on Computer Vision and Pattern Recognition*, 2021, pp. 7210–7219.
- [15] Quan Meng, Anpei Chen, Haimin Luo, Minye Wu, Hao Su, Lan Xu, Xuming He, and Jingyi Yu, “Gnerf: Gan-based neural radiance field without posed camera,” in *Proceedings of the IEEE/CVF International Conference on Computer Vision*, 2021, pp. 6351–6361.
- [16] Thomas Müller, Alex Evans, Christoph Schied, and Alexander Keller, “Instant neural graphics primitives with a multiresolution hash encoding,” *ACM Transactions on Graphics (ToG)*, vol. 41, no. 4, pp. 1–15, 2022.
- [17] Kai Zhang, Gernot Riegler, Noah Snaveley, and Vladlen Koltun, “Nerf++: Analyzing and improving neural radiance fields,” *arXiv preprint arXiv:2010.07492*, 2020.
- [18] Vincent Sitzmann, Julien Martel, Alexander Bergman, David Lindell, and Gordon Wetzstein, “Implicit neural representations with periodic activation functions,” *Advances in Neural Information Processing Systems*, vol. 33, pp. 7462–7473, 2020.
- [19] Emilien Dupont, Adam Goliński, Milad Alizadeh, Yee Whye Teh, and Arnaud Doucet, “Coin: Compression with implicit neural representations,” *arXiv preprint arXiv:2103.03123*, 2021.
- [20] Yannick Strümpfer, Janis Postels, Ren Yang, Luc Van Gool, and Federico Tombari, “Implicit neural representations for image compression,” in *European Conference on Computer Vision*. Springer, 2022, pp. 74–91.
- [21] Emilien Dupont, Hrshikesh Loya, Milad Alizadeh, Adam Goliński, Yee Whye Teh, and Arnaud Doucet, “Coin++: Neural compression across modalities,” *arXiv preprint arXiv:2201.12904*, 2022.
- [22] Hao Chen, Bo He, Hanyu Wang, Yixuan Ren, Ser Nam Lim, and Abhinav Shrivastava, “Nerv: Neural representations for videos,” *Advances in Neural Information Processing Systems*, vol. 34, pp. 21557–21568, 2021.
- [23] Zizhang Li, Mengmeng Wang, Huaijin Pi, Kechun Xu, Jianbiao Mei, and Yong Liu, “E-nerv: Expedite neural video representation with disentangled spatial-temporal context,” in *European Conference on Computer Vision*. Springer, 2022, pp. 267–284.
- [24] Yunpeng Bai, Chao Dong, Cairong Wang, and Chun Yuan, “Ps-nerv: Patch-wise stylized neural representations for videos,” in *2023 IEEE International Conference on Image Processing (ICIP)*. IEEE, 2023, pp. 41–45.
- [25] Joo Chan Lee, Daniel Rho, Jong Hwan Ko, and Eunbyung Park, “Ffnerv: Flow-guided frame-wise neural representations for videos,” *arXiv preprint arXiv:2212.12294*, 2022.
- [26] Hao Chen, Matthew Gwilliam, Ser-Nam Lim, and Abhinav Shrivastava, “Hnerv: A hybrid neural representation for videos,” in *Proceedings of the IEEE/CVF Conference on Computer Vision and Pattern Recognition*, 2023, pp. 10270–10279.
- [27] Ho Man Kwan, Ge Gao, Fan Zhang, Andrew Gower, and David Bull, “Hinerv: Video compression with hierarchical encoding based neural representation,” *arXiv preprint arXiv:2306.09818*, 2023.
- [28] Shishira R Maiya, Sharath Girish, Max Ehrlich, Hanyu Wang, Kwot Sin Lee, Patrick Poirson, Pengxiang Wu, Chen Wang, and Abhinav Shrivastava, “Nirvana: Neural implicit representations of videos with adaptive networks and autoregressive patch-wise modeling,” in *Proceedings of the IEEE/CVF Conference on Computer Vision and Pattern Recognition*, 2023, pp. 14378–14387.
- [29] Ze Liu, Yutong Lin, Yue Cao, Han Hu, Yixuan Wei, Zheng Zhang, Stephen Lin, and Baining Guo, “Swin transformer: Hierarchical vision transformer using shifted windows,” in *Proceedings of the IEEE/CVF International Conference on Computer Vision*, 2021, pp. 10012–10022.
- [30] Pruning Tutorial, “Tutorial for 11 unstructured pruning. https://pytorch.org/tutorials/intermediate/pruning_tutorial.html,”.
- [31] Alistair Moffat, “Huffman coding,” *ACM Computing Surveys (CSUR)*, vol. 52, no. 4, pp. 1–35, 2019.
- [32] Jorma Rissanen and Glen G Langdon, “Arithmetic coding,” *IBM Journal of research and development*, vol. 23, no. 2, pp. 149–162, 1979.
- [33] Alexandre Mercat, Marko Viitanen, and Jarno Vanne, “Uvg dataset: 50/120fps 4k sequences for video codec analysis and development,” in *Proceedings of the 11th ACM Multimedia Systems Conference*, 2020, pp. 297–302.
- [34] Haiqiang Wang, Weihao Gan, Sudeng Hu, Joe Yuchieh Lin, Lina Jin, Longguang Song, Ping Wang, Ioannis Katsavounidis, Anne Aaron, and C-C Jay Kuo, “Mcl-jcv: a jnd-based h.264/avc video quality assessment dataset,” in *2016 IEEE international conference on image processing (ICIP)*. IEEE, 2016, pp. 1509–1513.
- [35] Bunny scikit video, “scikit-video: video processing in python— scikit-video 1.0.0 documentation. <http://www.scikit-video.org/stable/datasets.html>,”.
- [36] Gisle Bjontegaard, “Calculation of average psnr differences between rd-curves,” *ITU SG16 Doc. VCEG-M33*, 2001.